

## DESIGN OF THE SC LASER DRIVEN INJECTOR FOR ARES

L.Serafini, P.Michelato, C.Pagani and A.Peretti

INFN and Universita' di Milano, Via Celoria 16, 20133 Milano, Italy

**Abstract**

The design of the superconducting laser driven RF gun for the ARES linac<sup>[1]</sup> is presented, as outlined according to the numerical simulations performed with the PIC code ITACA<sup>[2]</sup>. A new method to compensate the emittance increase induced by RF fields is also presented. The calculated performances of the injector system gives an electron beam brightness in excess of  $1.5 \cdot 10^{11}$  A/m<sup>2</sup>.rad<sup>2</sup>.

**Introduction**

A big effort has been done for some years in several laboratories to design and build electron sources capable to deliver high current beams with low transverse normalized emittance (in the range  $5 \cdot 10$  mm mrad<sup>[3,4,5]</sup>). In the context of the ARES project one of the primary goal is the production of high quality beams at high repetition rate in order to make possible both X-UV FEL<sup>[6,13]</sup> experiments and accelerator physics experiments in the main-streams of the  $\Phi$ -B Factories and TeV colliders<sup>[7]</sup> development. The low RF frequency (500 MHz) selected for the SC cavities of the LINAC constitutes, in this sense, a basic choice to assure a good beam quality (lower RF and wake-field induced effects, i.e. lower deteriorations of the beam dynamics properties through the acceleration).

The injector system for the LINAC must be compatible to this choice. A design based on a superconducting RF gun equipped with a laser driven photocathode becomes, in our opinion, mandatory to satisfy the requirements on the repetition rate and on the beam quality.

Our strategy to attain high peak current levels with short bunches is to extract from the gun relatively long bunches at low current and magnetically compress them when the energy is sufficient to avoid a further emittance increase due to space charge forces. Therefore a magnetic compressor must be foreseen to grow up the peak current to the level of some hundreds of Ampères: the current delivered by the SC RF gun cannot be in fact higher than a few tens of Ampères if the norm. emittance at the injector exit must be kept below a few mm-mrad. It is important to notice that the gun must provide excellent beam properties not only in the transverse phase space but also in the longitudinal one, since non-linearities in this space affect the full exploitation of the magnetic compression and limit the peak current at the exit of the injector.

**The injector design**

A schematic layout of the injection system is presented in fig.1

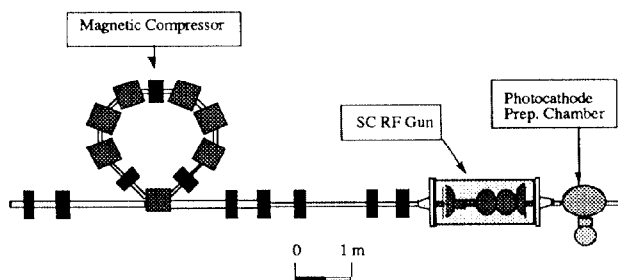


Fig. 1 - Schematic drawing of the superconducting RF injector. Magnetic compressor and photocathode preparation chamber are also shown

The requirements on the laser system and on the photocathode characteristics are summarized in Table 1, for the two selected bunch charges, which are representative of a high repetition rate high brightness beam (short bunches of .5 nC charge) and of a high charge low repetition rate beam (20 nC bunch charge).

Table 1 - Laser and photocathode requirements

Bunch charge	[nC]	.5	20
Peak current density	[A/cm <sup>2</sup> ]	80	520
Laser pulse length (rms)	[ps]	20	40
Laser peak power	[kW]	8.7	175
Laser pulse energy	[J]	$1.7 \cdot 10^{-7}$	$7 \cdot 10^{-6}$
Repetition rate	[Hz]	1000	30

Alkali semiconductors photoemitters and particularly cesium antimonide Cs<sub>3</sub>Sb photocathodes will be first investigated for the ARES gun. This material is easier to produce then composed alkali antimonide photoemitters (e.g. Na<sub>2</sub>K<sub>3</sub>Sb Cs) and it is characterized by an high quantum efficiency (about 1 %) and by a relative low sensitivity to the residual gas contamination. Nevertheless preparation chamber vacuum conditions are critical: total pressure must be in the low  $10^{-10}$  mbar range, with oxygen, nitrogen and carbon dioxide partial pressures in the  $10^{-12}$  mbar range. We expect that the clean environment of the gun SC cavity will increase the photocathode lifetime.

The laser system for the ARES injector is based on a mode-locked CW Nd:YLF laser as described elsewhere<sup>[1]</sup>.

**Results of the numerical simulations**

The modelling of a laser driven RF gun and the study of the associated beam dynamics require numerical simulation methods capable to describe the whole complex of processes which take place along the bunch acceleration. One of the most relevant for the beam dynamics is the interaction between the electrons and their e.m. self-field, which is in turn influenced by the interaction of this e.m. field with the RF gun cavity walls.

A self-consistent PIC code is needed if the wake field induced effects must be taken into account. Nevertheless, the field and particle integration algorithm and the assignment algorithm for the current and charge densities must minimize the associated unphysical fluctuations, which generate unphysical fields. Since the emittance is very sensitive to a straggling of the particle coordinates in the phase space, all kind of noise in the particle dynamics integration gives unphysical results for the beam emittance at the gun exit.

The code ITACA<sup>[2]</sup> applies a fourth order integration algorithm for the particle motion and the special Rician assignment algorithm for the bunch current<sup>[8]</sup>, obtaining a fluctuations free evolution both for the e.m. field propagation and for the particles motion.

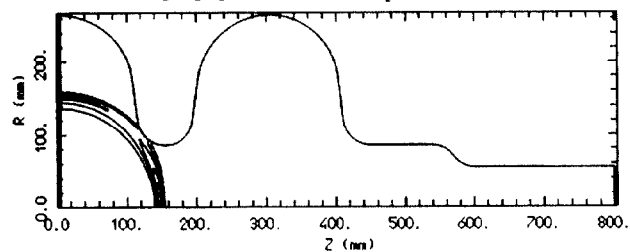


Fig.2 - Bunch self-field in the RF gun cavity

As an example, the wake field associated to a .5 nC bunch is shown in Fig.2, .56 ns after the photoemission from the photocathode, which is located at the center of the first half cell. The self-field has been obtained subtracting the fundamental  $TM_{010-\pi}$  mode from the total field, which is discretized over a regular mesh of  $6 \cdot 10^5$  points (maximum frequency carried by the mesh 230 GHz). The magnetic part of the self field is represented in fig.1 plotting the  $rH_\theta = \text{const.}$  lines, whereas the electric field components are shown in fig.3, where  $E_r$  and  $E_z$  are plotted as functions of  $z$  at some radii, within the mesh region around the bunch. No fluctuations are visible, although the self field gives a small contribution to the total field which is integrated in time over the mesh: the longitudinal electric field in the wake produced by the bunch is of the order of only a few kV/m, to be compared with the 30 MV/m of the peak RF electric field.

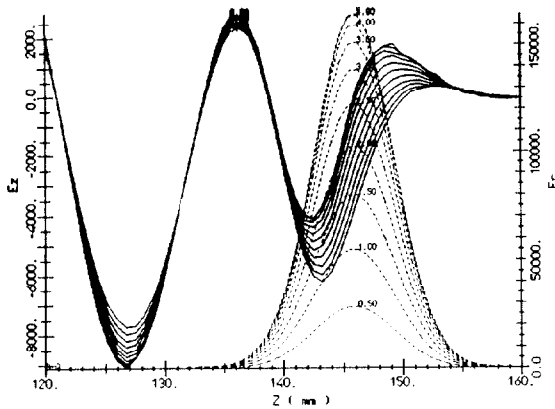


Fig.3 - Electric components of the bunch self-field (units V/m)

The absence of noise in the field integration is mainly due to the absence of fluctuations in the current densities, as shown in fig.4, where the longitudinal and transverse current densities of the .5 nC bunch are plotted as functions of  $z$  along the mesh lines ( $r$  varying from 0 up to 10 mm). As discussed elsewhere<sup>[1,8,11]</sup>, the unphysical fluctuations are negligible and the current distribution is still gaussian.

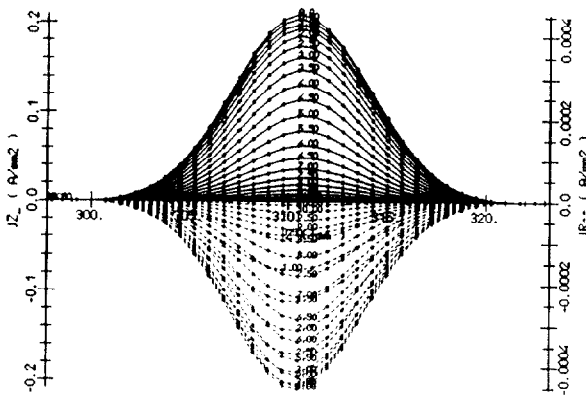


Fig.4 - Current density distributions of the .5 nC bunch.

The RF gun cavity geometry has been optimized to reduce the ratio between the maximum electric field on the iris and the peak field on the cathode, which is in our case 1.08, versus a ratio 1.28 for the LEP-like geometry which has been the starting point of our optimization. A larger radius of curvature for the iris allow to minimize the non-linear transverse RF field components. Also the ratio between the peak field on the cathode and the maximum magnetic field on the cavity walls has been minimized, achieving 1.7 kA/m per 1 MV/m. With high thermal conductivity niobium one can achieve up to 80 kA/m<sup>[10]</sup> of surface magnetic field, allowing to envisage a peak field on the cathode in the range of 40 MV/m. In our calculations we took a conservative value of 30 MV/m. The

resonating frequency of the  $TM_{010-\pi}$  mode is 499.5 MHz, while the unflatness of the axis electric field in the two cells is 1.5%.

The injection phase minimizing the RF induced emittance increase<sup>[9]</sup> is  $64^\circ$  RF for the .5 nC bunch. The normalized transverse emittance at the gun exit is 5 mm-mrad, but the longitudinal phase space exhibits a serious curvature, as shown in fig.5, where the phase space at the gun exit is shown together with the phase space at the exit of the magnetic compressor. The compression gives only a peak current increase by a factor five, from 20 up to 100 A. Higher injection phases gives more linear phase spaces, but larger emittances, in excess of 10 mm-mrad.

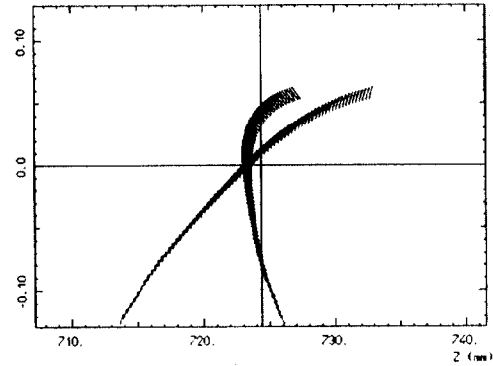


Fig.5 - Longitudinal phase space for the .5 nC bunch injected at the minimum emittance injection phase,  $64^\circ$  RF, at the gun exit (a) and after the magnetic compressor (b).

### Recovery of the RF induced emittance increase

The injection phase of a RF gun is always fixed to the value which minimize the RF induced  $\Delta p_r$ : the phase dependence of the momentum transfer is the basic mechanism producing the emittance increase<sup>[9]</sup>.

We studied a decoupled cell, as a possible time dependent RF lens, looking at the possibility to recover the RF induced emittance increase generated by the gun. We found that only an unsymmetrical cavity is able to generate a transverse momentum transfer  $\Delta p_r$  which is phase dependent.

The geometry of the decoupled cell is shown in fig.6: the cell is fully decoupled and independently phasable with respect to the gun cavity. The normalized emittance of a .5 nC bunch injected at  $80^\circ$  RF from the cathode is plotted in the same figure (dashed line): the emittance at the gun exit is 11 mm mrad, while at the decoupled cell exit the minimum value of 5 mm mrad is recovered. The strong modulations of the transverse emittance are due to the coupling between the longitudinal and the transverse phase spaces.

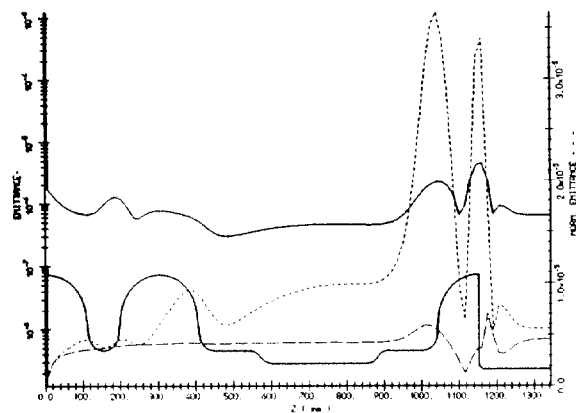


Fig.6 - Normalized (dotted line, scale on the right) and actual (solid line, scale on the left) transverse emittance of the .5 nC bunch, plotted along the acceleration through the whole RF gun + decoupled cell system. The dashed line on the bottom gives the norm. emittance of the central bunch core.

The emittance associated to the bunch central core (including the 10% of the charge) is actually free from modulations, and better exhibits the space charge contribution to the emittance increase, which is mainly produced in the first half cell of the gun.

Phasing properly the decoupled cell it is possible to achieve at the same time a nice focussing effect on the bunch, which leaves the cell with an rms divergence of 2 mrad, as shown in Fig. 7, where the transverse phase space at the gun exit and at the decoupled cell exit are plotted.

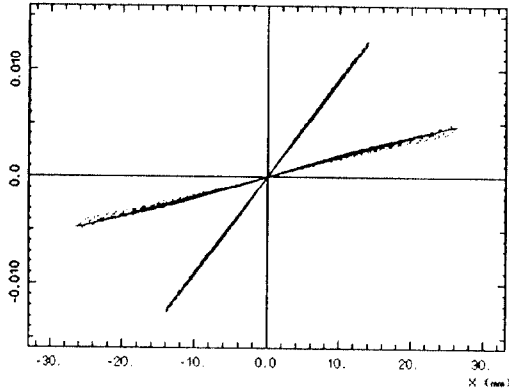


Fig. 7 - Transverse phase space at the gun exit (a) and at the cell exit (b).

Applying a longitudinal phase space transformation given, in TRANSPORT notation, by  $R_{56} = -0.8$  cm/percent, the magnetic compressor decreases the bunch length (rms) down to .2 mm, which corresponds to a peak current in excess of 400 A, with an associated brightness (defined according to ref.[3] as  $B_n = 2I / (4\pi\epsilon_n)^2$ )  $B_n = 1.8 \cdot 10^{11}$  A/m<sup>2</sup>rad<sup>2</sup>: the phase space transformation is shown in fig. 8.

The decoupled cell allows to increase the beam brightness by a factor four.

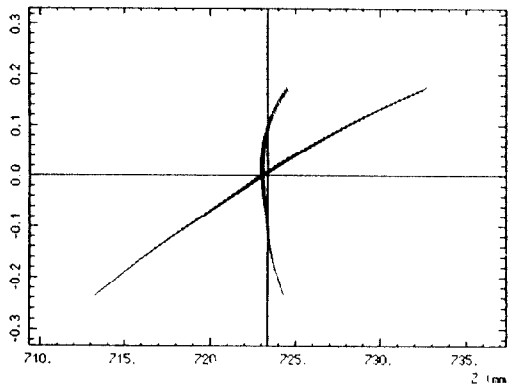


Fig. 8 - Longitudinal phase space of the .5 nC bunch at the exit of the decoupled cell (a) and after the magnetic compressor (b).

The RF gun is able to generate also high charged bunches, as shown in Table 2: the 20 nC bunch has a peak current at the gun exit of 350 A, which can be further compressed up to 2750 A, applying a  $R_{56} = -0.23$  cm/percent transformation. The maximum bunch radius at the exit is 27 mm and the rms divergence 15 mrad, fully compatible with the beam pipe size and the transport system.

We evaluated the emittance increase in the compressor by using the scaling law [12]  $\delta\epsilon_n = 6.9 I / \gamma^2$ , where  $\gamma$  is the beam energy in the compressor,  $I$  the current and  $\delta\epsilon_n$  the rms norm. emittance increase in mm-mrad. In order to keep the final emittance within 6 mm mrad, it is necessary to envisage a two stage compression, the first one at 8 MeV, from 20 up to 100 A, and the second at 20 MeV, from 100 up to 400 A. The two stage compressor is now under study: a 2+1/2 cell gun cavity has been already simulated in order to achieve a beam energy of 9 MeV at the exit of the decoupled cell (the emittance recovery by the decoupled cell requires a decelerating field,

with a 3 MeV energy decrease in the cell). The emittance at the exit of the system formed by the 2+1/2 cell gun and the decoupled cell is still 5 mm mrad, but the compressed peak current is slightly lower, at 350 A. A careful optimization of the decoupled cell is under way to minimize the induced curvature in the longitudinal phase space.

Table 2 SC RF gun performances

	A	B	
Bunch charge (nC)	.5	.5	20
Laser spot ( $\sigma_r$ ) (mm)	2.	2.	3.5
Laser pulse rms length ( $2\sigma_L$ ) (ps)	20	20	40
RF injection phase (deg)	64	80	75
Output energy (MeV)	7.4	3.8	6.8
Rms energy spread (keV)	$\pm 28$	$\pm 34$	$\pm 195$
Rms bunch radius $\sigma_x$ (mm)	6.2	12.7	15.
Rms bunch length (mm)	5.8	6.3	12.5
Rms divergence $\sigma_{x'}$ (mrad)	5.8	2.4	15.3
Rms transv. emitt. $\epsilon_n$ (mm-mrad)	5.9	5.5	106
Peak current (no compr.) (A)	19	18.5	350
Peak current (magn. compr.) (A)	125	435	2750
Norm. brightness ( $10^{11}$ A/m <sup>2</sup> rad <sup>2</sup> )	.45	1.8	.03

A: at the gun exit, without the decoupled cell. B: at the exit of the decoupled cell

## Conclusions

We have shown that a low frequency SC RF gun can be designed to produce high brightness beams at high repetition rate. The new proposed method for the recovery of the RF induced emittance increase allows to attain high peak current levels (400 A) with low normalized transverse emittance (5 mm-mrad).

## References

- [1] The ARES superconducting LINAC, rep. INFN LNF-90/035 (R) and "The ARES project", Proc. of this conference.
- [2] L.Serafini and C.Pagani, "ITACA: a computer code for the integration of transient particle and field equations in Axisymmetrical cavities", Proc. 1<sup>st</sup> EPAC, Rome, 1988, p.866
- [3] J.S.Fraser and R.L.Sheffield, IEEE of Q. Electronics, QE-23, 9, 1987, p.1489.
- [4] R.L.Sheffield, Proc. of the 1989 IEEE Part. Acc. Conf., IEEE cat. 89CH2669-0, p.1098
- [5] X.J.Wang et al., Proc. of the 1989 IEEE Part. Acc. Conf., IEEE cat. 89CH2669-0, p.307
- [6] J.C.Goldstein, Proc. of the ICFA workshop on low emitt. e<sup>-</sup>e<sup>+</sup> beams, BNL 52090 UC-28, 1987, p.180.
- [7] R.Sundelin, "Fully superconducting linear colliders", Proc. Capri workshop on linear colliders, Capri, June 1988.
- [8] A.Peretti, L.Serafini and M.Zanin, "The Rician assignment algorithm for PIC codes", to be published
- [9] K.J.Kim, NIM, A275 (1989), p.201.
- [10] H.Chaloupka et al., Proc. of the 4<sup>th</sup> work. on RF Superconductivity, 1989, Tsukuba, KEK rep. 89-21, p.583.
- [11] L.Serafini et al, "Numerical simulations for the ARES SC injector", rep. INFN TC-90/10
- [12] T.I.Smith, Proc. of the ICFA workshop on low emitt. e<sup>-</sup>e<sup>+</sup> beams, BNL 52090 UC-28, 1987, p.125.
- [13] L.Serafini et al., "Sub-harmonic optical klystron", rep. INFN TC-90/11, 1990